ELSEVIER

Chemometrics and Intelligent Laboratory Systems 60 (2002) 135–146

Chemometrics and intelligent laboratory systems

www.elsevier.com/locate/chemometrics

Multi-way analysis of trace elements in fish otoliths to track migratory patterns

Paul J. Gemperline [a,*], Roger A. Rulifson [b], Lee Paramore [b,1]

[a] *Department of Chemistry, College of Arts and Sciences, East Carolina University, 205 Flanagan, Greenville, NC 27858, USA*
[b] *Department of Biology, and Institute for Coastal and Marine Resources, East Carolina University, Greenville, NC 27858, USA*

Abstract

Spawning striped bass in the Shubenacadie watershed of Nova Scotia, Canada exhibit three dorsal coloration patterns: green, indicative of fish from the ocean; black, indicative of fish that overwinter in a fresh headwater lake, and mottled fish of unknown origin. Microchemical analysis of growth rings in fish otoliths (calcareous particles found in the inner ear of certain lower vertebrates), measured by laser ablation-inductively coupled plasma/mass spectrometry (LA-ICP/MS), from fish captured during the 1999 Shubenacadie spawning period were analyzed by Tucker-3 multi-way principal component models. Using this technique, multidimensional patterns were discovered in the trace element measurements indicating that migratory patterns of individual striped bass can be tracked from the time-dependent trace element record deposited in the otoliths. Of the nine fish analyzed by LA-ICP/MS, trace element composition at year 0 suggested that all nine fish originated from the same locale. Differentiation in the trace element record was observed in subsequent years. Clustering of the trace element data for six fish unambiguously coincided with dorsal coloration. The three remaining fish exhibited trace element patterns that suggested migration between freshwater and marine conditions at one or more periods during life.

Keywords: Otoliths; Shubenacadie watershed; Migratory patterns; Striped bass; *Morone saxatilis*

1. Introduction

Striped bass, *Morone saxatilis*, is an important commercial and recreational species along the North American Atlantic coast. Populations north of Cape Hatteras, NC spawn in fresh or brackish waters in the spring and return to coastal ocean waters. Juveniles tend to stay in brackish coastal waters until 1–2 years of age, then enter the ocean and participate in coastal migrations [1].

Striped bass populations occurred in three regions of Atlantic Canada: The St. Lawrence River and estuary in Quebec; the Gulf of St. Lawrence, specifically rivers of Eastern New Brunswick; and the Bay of Fundy from the St. Croix River in New Brunswick to the Tusket River in Nova Scotia [1]. These populations in Atlantic Canada have declined dramatically in recent years [2]. The spawning population in the St. Lawrence River was apparently decimated in the 1960s [3] and was possibly extinct by 1966 [4]. The species was declared endangered in Quebec province in 1984 [4]. Recent declines in the popula-

* Corresponding author. Tel.: +1-252-328-6767; fax: +1-252-328-6210.
E-mail address: gemperlinep@mail.ecu.edu (P.J. Gemperline).
[1] Present address: North Carolina Division of Marine Fisheries, PO Box 539, Wanchese, NC 27981, USA.

0169-7439/02/$ - see front matter
PII: S0169-7439(01)00191-5

tion of striped bass in the Gulf of St. Lawrence prompted federal regulators to restrict capture to hook and release by anglers. Only two rivers now support self-sustaining populations in Atlantic Canada [2], one of which is the Shubenacadie River at the head of the Bay of Fundy. Spawning occurs 3–6 km upriver of the Shubenacadie River–Stewiacke River confluence (see Fig. 1).

The Shubenacadie River is a tidal bore river with environmentally harsh conditions due to tidal surges that can change the water quality dramatically within minutes. The height of the tidal bore wave front varies between 0.2 and 0.5 m on neap and spring tides, respectively. Spring tides can cause changes in the Stewiacke River depth of up to 3.7 m within 1 h with a concomitant change in water quality including fluctuations in salinity (0–19.2‰), temperature (11.0–14.7 °C) and dissolved oxygen levels (8.0–10.6 mg/l) [2].

Adult striped bass overwintering in the ice-covered Shubenacadie Lake have black dorsal coloration and are called "blackback" fish by local fisherman. These fish begin downstream migration in the first week of May. Striped bass migrating upstream from seaward have a green dorsal coloration and are called "greenback" fish by local fishermen. These fish begin an upstream migration in April and meet the downstream migrants in the third week of May at the confluence of the Shubenacadie and Stewiacke Rivers, near the head of the salt wedge (see Fig. 2) [2]. It is not known if individuals belonging to these different groups maintain one of the two patterns throughout life, or switch between fresh or marine overwintering habitats.

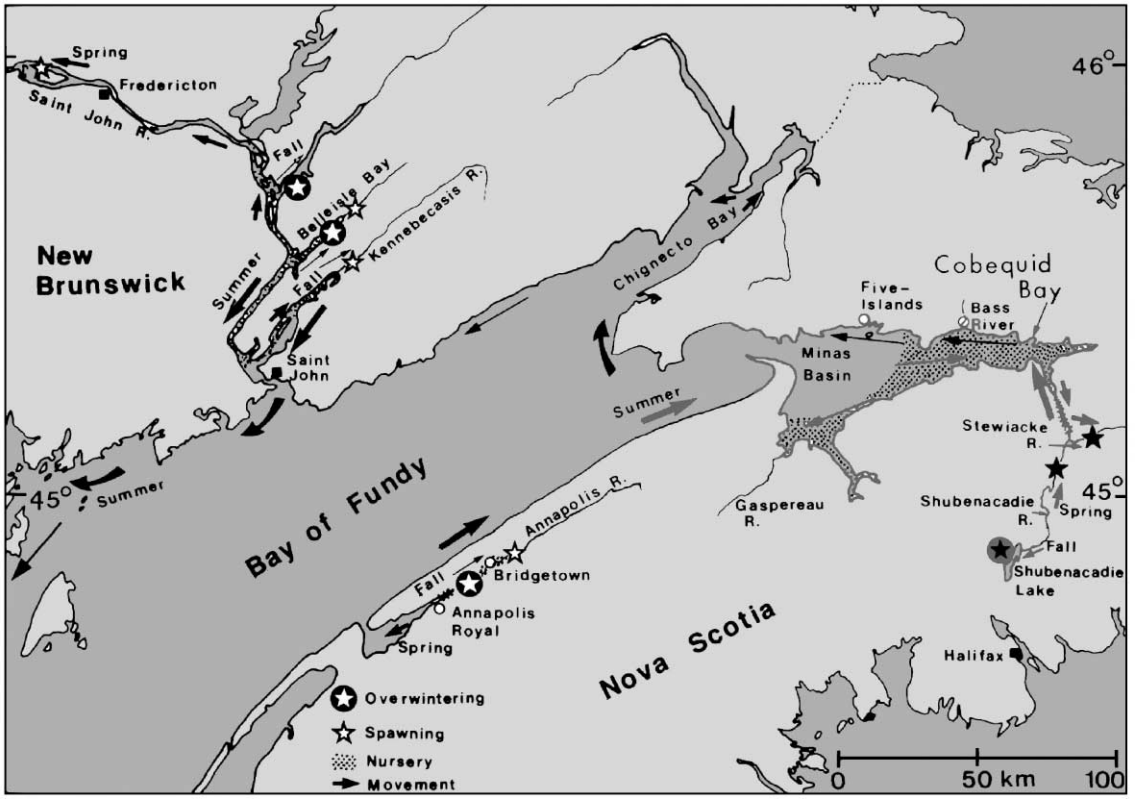

Fig. 1. Overwintering sites, known and possible spawning sites, nursery areas, and seasonal movements of striped bass in the Bay of Fundy region: Annapolis and Shubenacadie Rivers, Nova Scotia, and the Saint John River, New Brunswick [1]. Only the Shubenacadie watershed supports a spawning, self-sustaining population at this time.

1.1. Otolith microchemistry

Numerous studies of trace elements in otoliths have demonstrated that physiology [5], age [6], and environment [7] affect otolith composition (calcareous particles found in the inner ear of certain lower vertebrates). Annual growth rings appear in the calcareous otolith matrix (see Fig. 2). Opaque layers are formed during periods of slow growth and translucent layers are formed during periods of rapid growth (spring and summer). These growth rings provide a long-term record of the life history of fish by incorporating elemental differences in water chemistry found in different water bodies [8–10]. Otoliths provide a permanent record because they are physiologically static accumulations of calcareous material and are at no point reabsorbed [11]. Several research groups have studied Sr/Ca ratios in otoliths to study the life history of different species as they migrate from freshwater to brackish or saltwater environments [12–20].

1.2. Multivariate analysis

Traditionally, univariance methods of analysis have been used to study trace elements in fish otoliths. Most frequently, analysis of variance (ANOVA) has been used to discover statistically significant variation in different trace elements. Trends in trace element composition are frequently studied by examining plots as a function of time or by plotting univariant distributions by year. These approaches neglect the possibility that there may be correlations by age, by element, and by fish. A few authors have employed two-way methods of analysis including linear discriminant analysis, multiple analysis of variance (MANOVA), conconical analysis of variance, and artificial neural networks for classification [21–26].

Traditional two-way methods of analysis can simultaneously consider correlation in two modes of a data array; for example, correlation among individuals (fish) and correlation among elements. Often, however, three or more modes may be available for analysis. For example, in the present study, trace elements can be organized into a three-way array consisting of (individuals × elements × age). Currently, there are three well-known methods of analysis that are suitable for analysis of three-way arrays. These include the Tucker-3 decomposition [27], which is a generalization of principal component analysis to multi-way arrays, and two equivalent methods called PARAFAC, and CANDECOMP,

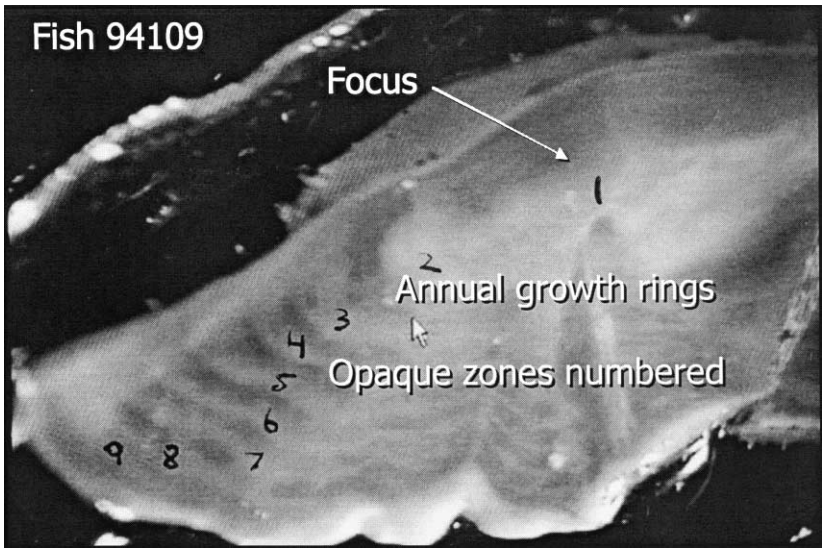

Fig. 2. Saggital section of a typical otolith showing the primordium (focus) and annual growth rings. Laser microsampling sites in the opaque zones (slow growth regions) are numbered.

introduced simultaneously by Harshman [28] and by Carol and Chang [29], respectively. Principal component analysis of two-way arrays offers significant advantages compared to univariate techniques, in that it properly treats correlated behavior between two or more variables. Because of the power of this approach, the technique has become very popular during the past two decades [30]. Principal component analysis of a three-way data array offers similar advantages on a greater scale and has received increased attention in the chemometrics literature [31–35].

Trace element measurements were organized into a three-way data array prior to fitting of the Tucker-3 principal component model used in this study. Individual fish were arranged as rows in the data array and grouped according to their dorsal coloration: greenback, blackback, or uncertain. Columns in the data array represent background corrected counts of different isotope ratios, and slices of the data cube represent trace element composition of these fish at different ages based on samples taken from different annual growth rings in the otoliths. The Tucker-3 model is comprised of three matrices of eigenvectors, one for each mode in the original array, where **G** is a matrix of eigenvectors representing the relationship among individual fish, **H** is a matrix of eigenvectors representing the relationships among individual trace elements, and **E** is a matrix of eigenvectors representing the relationship among different ages of fish. The elements of the core matrix are analogous to eigenvalues in a standard two-way principal component model. The magnitude of an element, C_{pqr}, describes the magnitude of the information modeled by the triad of eigenvectors $\mathbf{g}_p$, $\mathbf{h}_q$ and $\mathbf{e}_r$. Large absolute values of the core elements indicate that the corresponding vectors of **G**, **H**, and **E** describe a large fraction of the variance in the original data, whereas small values indicate that corresponding vectors of **G**, **H**, and **E** describe small amounts of variance in the original data table. Eq. (1) describes how the individual elements of these matrices are multiplied together to model an individual measurement, D_{ijk}

$$D_{ijk} = \sum_{p=1}^{s} \sum_{q=1}^{t} \sum_{r=1}^{u} \mathbf{g}_{ip}\mathbf{h}_{jq}\mathbf{e}_{kr}c_{pqr} + \mathbf{E}_{ijk}. \quad (1)$$

Kroonenberg and de Leeuw [36] developed a nonlinear iterative algorithm for minimizing the sum of squares represented in Eq. (2).

$$\min\left(\sum_{i=1}^{l}\sum_{j=1}^{m}\sum_{k=1}^{n}\left(D_{ijk} - \sum_{p=1}^{s}\sum_{q=1}^{t}\sum_{r=1}^{u}\mathbf{g}_{ip}\mathbf{h}_{jq}\mathbf{e}_{kr}c_{pqr}\right)^2\right). \quad (2)$$

The details of the alternating least squares algorithm and proof of convergence [37] are beyond the scope of this paper; however, some important properties of the solution are discussed. Firstly, columns of **G**, **H**, and **E** are mutually orthogonal and normalized, which makes the results of the model easy to interpret graphically. The total variance explained by **G**, **H**, and **E** can be determined from the eigenvalues of **G**, **H**, and **E**. Additionally, the total variance explained by the Tucker-3 model can be partitioned into two parts as shown in Eq. (3)

$$ss_{\text{tot}} = ss_{\text{fit}} + ss_{\text{res}} \quad (3)$$

where ss_{tot} is the total sum of squares for array **D**, ss_{fit} is the total sum of squares described by theTucker-3 model, and ss_{res} is the residual sum of squares. In this paper, global mean centering was applied to columns (trace elements) prior to fitting the Tucker-3 model.

2. Experimental

Otoliths used in this study were taken from a few selected fish that were collected as part of a study previously reported [38]. During this study, a local commercial fishery fleet of part-time gill net fishers targeting American shad, *Alosa sapidissima*, and alewife, *A. pseudoharengus*, caught and marketed striped bass through the local fish house. A total of five blackbacks and four greenbacks ranging from 7 to 10 years in age were selected. The fishermen performed color classifications, all of which were unambiguous. The number of fish selected was small due to the cost of performing microchemical analysis and budget constraints.

Sagittal otoliths were removed, washed, dried, and weighed. Transverse cut sections from each otolith were glued to microscope slides and polished by wet sanding with emery paper to expose the otolith primordium and annular rings. Polished otoliths were

sonicated in triple D water (double distilled deionized water) and stored for analysis by laser ablation-inductively coupled plasma/mass spectrometry (LA-ICP/MS). Each otolith section was placed in the sample apparatus and the laser was focused on the central core. The target sample locations were the opaque and translucent zones in a linear transact from the otolith focus to the outer edge (see Fig. 2). Up to 18 samples were measured for each otolith. In some cases, only a limited number of samples were taken, and some growth rings were skipped because they could not be easily identified in the microscopic image.

An argon gas blank was used to determine background levels for each isotope. Sixty-second laser pulses were used to ablate material, which was then swept into the ICP/MS by argon gas. A Q-switched Nd/YAG laser at either 355 or 532 nm with a beam diameter of 15–20 μm was used. The isotopes sampled by ICP/MS are listed in Table 1.

3. Results and discussion

Output from the LA-ICP/MS analysis, in counts per second, was corrected for the blank values

A)

Age	0	1		2		3		4		5		6		7		8		9		10						
Ring	F	C	O	C	O	C	O	C	O	C	O	C	O	C	O	C	O	C	O	C	O	C				
FISH	Color	SHOT #:																					GROUP:		
94041	G	1		2	3	4	5	6	7	8	9	10	11	12	13	14							O	C	OC
94160	G	1	2	3	4	5	6	7	8	9	10	11	12	13	14	15	16	17	18				O	C	OC
94192	G		1		2		3		4		5		6		7		8		9					C	
94195	G				1		2		3		4		5		6		7		8		9	10		C	
94193	B	1		2	3	4	5	6	7	8	9	10	11	12	13	14	15						O	C	OC
94046	B		1	2	3	4	5	6	7	8	9	10	11	12	13								O	C	OC
94136	B			1	2	3	4	5	6	7	8	9	10										O	C	
94109	B	1		2		3		4		5		6		7		8		9					O		
94188	B		1		2		3		4		5		6		7		8		9		10			C	

B)

94041	G		2		4		6		8		10						O	
94160	G		3		5		7		9		11						O	
94192	G		2		3		4		5		6						C	
94195	G		1		2		3		4		5						C	
94193	B		2		4		6		8		10						O	
94046	B		2		4		6		8		10						O	
94136	B		1		3		5		7		9						O	
94109	B		2		3		4		5		6						O	
94188	B		2		3		4		5		6						C	

C)

94041	G			3		5		7		9		11					C	
94160	G			4		6		8		10		12					C	
94192	G			2		3		4		5		6					C	
94195	G			1		2		3		4		5					C	
94193	B			3		5		7		9		11					C	
94046	B			3		5		7		9		11					C	
94136	B			2		4		6		8		10					C	
94109	B			2		3		4		5		6					O	
94188	B			2		3		4		5		6					C	

Fig. 3. (A) Pattern of annual growth rings sampled by age and by fish. (B) Reconstructed set of nine fish obtained by substituting shots in adjacent clear layers for missing shots in adjacent opaque layers. (C) Reconstructed set of nine fish obtained by substituting shots in adjacent opaque layers for missing shots in adjacent clear layers. (F) = shot taken in the otolith focus or primordium. (C) = shot taken in a clear or translucent portion of the otolith annular ring. (O) = shot taken in an opaque portion of the otolith annular ring.

recorded before each otolith sample. The resulting blank corrected data were normalized to remove sample-to-sample intensity fluctuations by dividing by ^{48}Ca intensity in counts per second. Previous studies demonstrated ^{48}Ca is a good measure of ablated mass and is relatively invariant across otoliths sections [23]. The resulting collection of measurements is represented in Fig. 3, with missing shots shown as blank squares. A strategy was devised (described in detail later) to treat missing shots by substituting shots from adjacent clear or opaque layers. Prior to this treatment, a total of four fish—94041, 94160, (greenbacks) and 94193, 94046, (blackbacks)—with complete records of opaque and clear growth rings for a contiguous period of 6 years was studied by use of multivariate analysis of variance (MANOVA) to test for differences between clear and opaque layers in these four fish. Results of the analysis revealed that there was no significant difference ($p > 0.75$, $df = 34, 13$) in trace element composition between opaque and clear rings of otoliths.

The MANOVA results described above suggested that a complete record of nine fish over a period of 5 years could be constructed by replacing missing shots with data from a shot taken in an adjacent layer (see Fig. 3). Two complete sets of data were constructed using this strategy. The first set was constructed by replacing missing shots in opaque regions of fish 94192, 94195, and 94188 with shots measured in the clear region from the adjacent of increasing age (see Fig. 3). The second set was constructed in a similar fashion by replacing missing shots in the clear regions of fish 94109 with shots measured in the opaque region from the ring immediately preceding it in age (see Fig. 3).

Prior to fitting Tucker-3 models, uninformative variables were identified by one-way analysis of variance (ANOVA) and box plots. Isotopes with means not significantly different from zero ($p > 0.05$) were removed, leaving a total of 34 isotopes, representing 23 different elements for further analysis (see Table 1).

In a subsequent analysis of variance (results not shown), ^{46}Ca and ^{55}Mn had means significantly different by fish ($p < 0.05$), but had no significant difference ($p > 0.05$) by fish color or by year. By use of ANOVA, it was discovered that fish 94195 had significantly higher levels of lead, zinc, mercury, iodine, copper, iron and chromium in the clear layer of year 1 only. The fish had normal levels of the remaining isotopes in the clear zone of year 1, and normal levels of all isotopes in all remaining clear and opaque regions. Analysis of variance by fish color—

Table 1
Summary statistics for isotopes sampled by laser ablation ICP/MS in four fish with complete clear and opaque records over a period of 6 years

Variance	Used	Mean	Median	S.D.	Range
Li-6		−0.0002	−0.0028	0.0405	0.2185
Li-7		0.0010	−0.0184	0.1072	0.4569
Be-9		0.0024	0.0021	0.0124	0.0604
B-10	×	0.1360	0.1287	0.0419	0.2008
Mg-24	×	26.7025	22.9800	13.4993	62.4957
Mg-25	×	2.8407	1.9586	3.7384	25.0414
Mg-26	×	3.4282	2.5660	4.3129	29.2248
Al-27	×	3.7935	2.1019	6.3227	43.3403
S-34	×	256.3900	260.3910	41.8897	141.8010
Sc-45	×	2.0505	1.7279	1.1834	6.5549
Ca-46	×	17.9748	17.7936	1.2857	5.8797
Ca-48		1000.0000	1000.0000	0.0000	0.0000
Ti-49		0.1481	0.1002	0.1475	0.7050
V-51		0.0227	0.0231	0.0722	0.3923
Cr-52	×	41.1953	36.4241	10.9908	40.5902
Cr-53	×	0.4810	0.4510	0.1287	0.5413
Mn-55	×	12.5964	3.7029	17.6900	71.8746
Fe-57	×	1.0987	1.1508	0.6045	3.6541
Ni-58	×	0.1292	0.0950	0.2504	1.5442
Co-59		1.6466	1.5923	0.3390	1.5441
Cu-63	×	0.7358	0.5089	0.4915	1.7541
Cu-65	×	0.2551	0.1156	0.2688	1.1445
Zn-66	×	0.7347	0.5834	0.5728	2.8248
Zn-67	×	0.1473	0.1182	0.0976	0.5056
Zn-68	×	0.6076	0.5086	0.3813	2.0678
As-75	×	0.3523	0.0824	1.4658	10.2785
Rb-85	×	0.1510	0.0968	0.1432	0.8822
Sr-86	×	226.6240	263.4150	114.9560	336.7040
Sr-87	×	166.2220	194.1430	84.5045	243.7410
Cd-111	×	0.0359	0.0306	0.0338	0.1727
Cd-114	×	0.0821	0.0639	0.0664	0.3740
Sn-120	×	0.0327	0.0450	0.2667	2.0312
Sb-123		0.0175	0.0152	0.0207	0.1332
I-127	×	1.1427	1.1154	0.4031	1.8792
Ba-137	×	1.5511	0.8630	1.3472	4.1796
Ba-138	×	9.9727	5.6263	8.7144	26.7166
Ce-140	×	0.0082	0.0035	0.0157	0.0796
Hg-200	×	0.1231	0.1046	0.0928	0.5048
Hg-201		0.0726	0.0664	0.0552	0.3122
Hg-202	×	0.1624	0.1547	0.1067	0.5826
Pb-206	×	0.1730	0.0827	0.2021	1.0355
Pb-207	×	0.1416	0.0749	0.1914	1.1233
Pb-208	×	0.3556	0.1871	0.4534	2.5080

blackback or greenback—revealed unique response for ^{120}Sn. Other groups of variables showed significant variance by fish and by fish color. These included S, Cr, Co, Cu, Rb, Sr, Ba, and Ce. A surprising observation was that the ANOVA results showed there was no significant difference in the isotope mean values by age of fish. Graphical investigation of the isotope measurements using box plots by age of fish revealed trends by age of fish.

3.1. Tucker-3 analysis

All of the Tucker-3 results reported below were obtained using the reconstructed data set of all nine fish, aged 1 through 5, with missing data in opaque layers replaced using measurements from clear layers. The analyses were repeated using the data set with missing shots in clear layers replaced with data from opaque layers, and similar results were obtained. Since it is known that Tucker-3 models are sensitive to the choice of data centering and standardization techniques, several different schemes were tried, including global centering of columns, centering of columns by layers, global centering of columns and standardization of columns to unit variance, and centering and standardization of columns by layer. Scatter plots of fish (described later) had the same general appearance of clusters, regardless of the centering and standardization options selected, a consequence of the ^{48}Ca data normalization scheme used.

A Tucker-3 model using three factors for **G**, three factors for **H**, and four factors for **E** accounted for 86.0% of the variance in the original measurements. This model reduced the dimensionality of the isotope measurements from 34 to 3 orthogonal variables, reduced the dimensionality measurements by fish from 9 to 3, and reduced the dimensionality of measurements by age from 5 to 4. Table 2 lists the percent variance explained by each *I*, *J*, *K* triad of factors represented in the core matrix. Some of the most important triads of vectors can be observed in Table 2. The first triad, $\mathbf{g}_1\mathbf{h}_1\mathbf{e}_1$, accounted for 51.8% of the variance in the original measurements. This triad of factors was by far the most important, with the first column of **H** dominated by variance contributed by ^{86}Sr and ^{87}Sr, as observed by the magnitude of Sr scores in **H** (not shown). All nine fish contributed approximately equally to the first column of **G** and ages 1–4 contributed significantly to the first column of **E**, but a relatively small contribution is observed from year 5. Sulfur had the largest contribution of variance to the second column of **H** with minor contributions from ^{86}Sr, ^{87}Sr, and ^{52}Cr. In the third column of **H**, ^{24}Mg, ^{52}Cr, ^{55}Mn contributed a substantial amount of variance.

Table 2
Percentage of variance described by triads vectors, $\mathbf{g}_i\mathbf{h}_j\mathbf{e}_k$, in the Tucker-3 model of fish otolith trace element measurements

Rows of **H**	Columns of **G**		
	1	2	3
Layer 1 = 1st column of **E**			
1	51.781	0.579	0.014
2	0.062	0.011	0.020
3	0.269	0.193	0.280
*Layer 2 = 2nd column of **E***			
1	0.012	0.196	0.000
2	11.787	0.069	0.032
3	2.763	0.630	0.020
*Layer 3 = 3rd column of **E***			
1	0.194	1.686	0.103
2	2.898	0.555	0.001
3	6.119	1.361	0.017
*Layer 4 = 4th column of **E***			
1	0.014	3.295	0.015
2	0.035	0.016	0.002
3	0.910	0.027	0.043

A scatter plot of the isotopes was constructed using the first, second, and third columns of matrix **H** as *x*, *y*, and *z* plotting coordinates. Four groupings of isotopes were observed in the scatter plot (see Fig. 4). A cluster of 28 isotopes appeared near the origin. This indicated that the variance in the measurements of these 28 isotopes was small compared to Sr, S, Mg and Mn. The isotopes ^{86}Sr and ^{87}Sr formed a distinct cluster in this scatter plot as their responses were highly correlated, as expected. The isotope, ^{34}S, appeared to have a unique response different from the other isotopes found in Fig. 4. A cluster comprising the isotopes ^{52}Cr, ^{24}Mg and ^{55}Mn appeared aligned along the axis $\mathbf{H}_3$.

Different patterns were observed in this scatter plot when standardized data were used. With standardization of columns, each column was weighted so that it contributed equally to the Tucker-3 model. In this

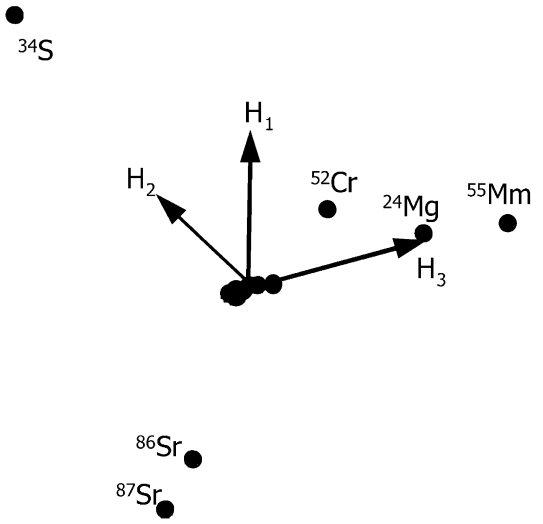

Fig. 4. Scatter plot of the first three columns of **H**, showing four groupings of isotopes.

case, some evidence of clustering of Hg, Pb, and Cd isotopes was observed as well as an additional cluster of As and Ce; however, neither were as distinctly identified as the clusters observed for non-standardized data.

The six important isotopes identified in Fig. 4 were further investigated by examining the distribution of measurements by fish color in histograms (see Fig. 5) and by examining the distribution of fish in these histograms. Clear trends were observed in the histograms for ^{52}Cr, and (^{86}Sr, ^{87}Sr) when greenback fish were highlighted in these plots (see Fig. 5). A strong negative correlation can be observed between Cr and Sr for greenback fish. Bimodal distributions were observed for Cr and Sr, which provided good separation between greenback and blackback fish when ignoring year 0 data.

Clustering by fish color was examined in scatter plots obtained by reducing the dimensionality of the data matrix projected into the subspace spanned by the first three columns of matrix **H** (see Fig. 6). In this scatter plot, blackback fish formed a cluster that was clearly separated from a cluster of greenback fish plus the 0 age data from blackback fish. Three fish—94192, 94188, and 94046—did not follow the expected pattern of trace elements and are not shown

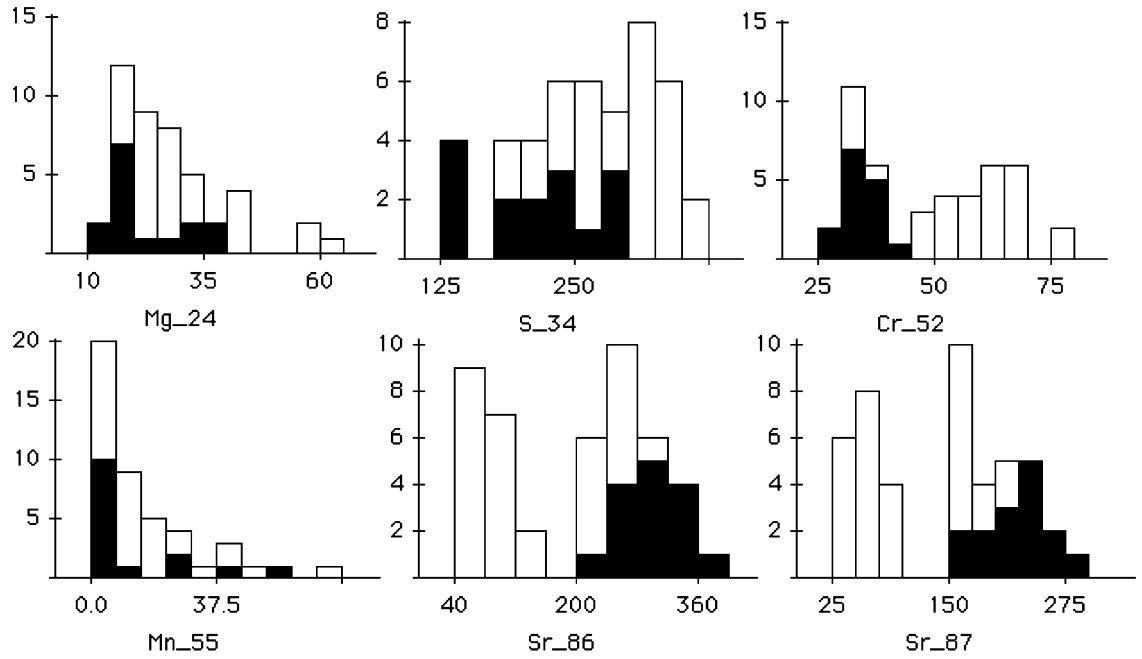

Fig. 5. Histograms showing the distribution of isotope measurements. White bars represent all fish. Black bars represent the distribution of greenback fish.

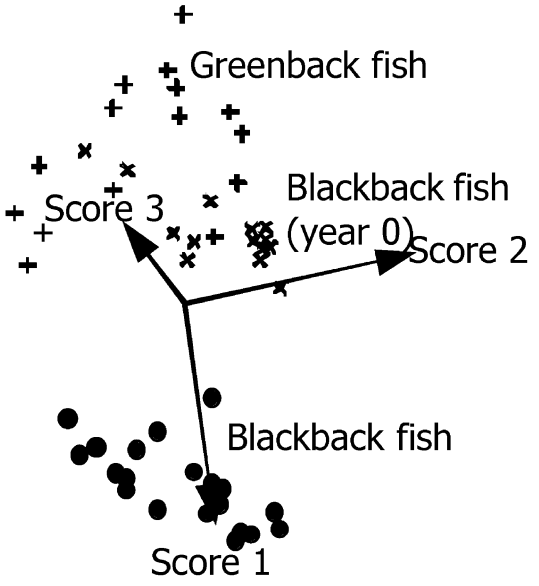

Fig. 6. Scatter plot showing the clusters of (●) blackback fish (ignoring age 0), (+) greenback fish, and (×) blackback fish at age 0.

in the scatter plot (described later). Age 0 data for blackback fish clustered with the data for greenback fish in Fig. 6. This suggests that blackback and greenback striped bass hatch and grow in the same environmental locale during the first year (age 0) of life, in good agreement with previous studies [1,2]. Typically, age 0 striped bass spend the summer and fall in brackish (mesohaline) nursery areas. After the first year of life, shifts in trace element patterns suggest that the two groups inhabit different environmental conditions, i.e. greenbacks overwinter in ocean habitats and blackbacks overwinter in freshwater habitats.

When plots of the first column of scores shown in Fig. 6 were constructed by age of fish, clearly visible trends were observed (see Fig. 7(A–D)). At age 0, all nine fish had scores comparable in magnitude. In subsequent years, blackback fish had higher values on score 1 compared to greenback fish (see Fig. 7(A)). In Fig. 7(B), fish 94192, classified as a greenback fish, had scores similar to greenback fish during years

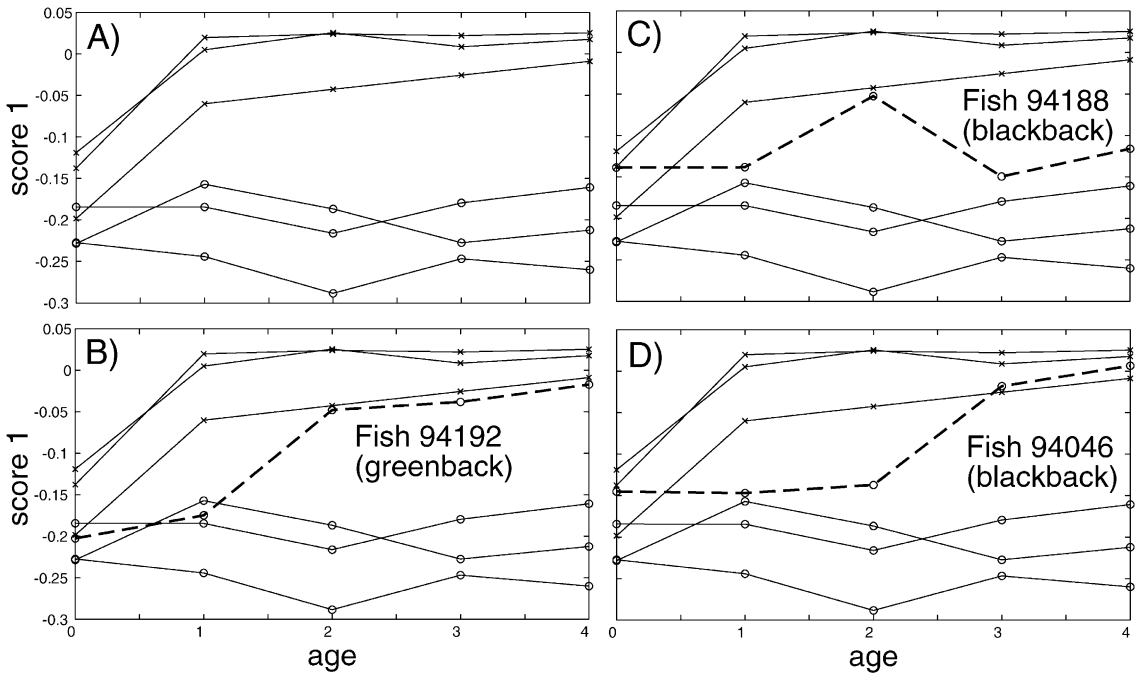

Fig. 7. Trends in scores by fish and age of fish. (A) Six unambiguously classified greenback fish (○), blackback fish (×). (B, C, and D) Evidence of habitat switching indicated by shifts in trace element patterns (– –).

0 and 1 of its life but in subsequent years, it had scores similar to blackback fish. Therefore, we hypothesize that this fish overwintered in a saltwater environment during years 0 and 1, but in subsequent years it switched and overwintered in the fresh headwater Shubenacadie Lake with blackback fish. In Fig. 7(C), fish 94188, originally classified as a blackback fish, had scores similar to greenback fish at age 0, 1, 3, and 4. These results suggest that this fish overwintered with blackback fish at age 2. In Fig. 7(D), fish 94046, originally classified as a blackback fish, had scores similar to greenback fish at age 0, 1, and 2. At age 3 and 4, this fish likely overwintered with blackback fish in a freshwater environment.

Paramore and Rulifson [38] hypothesized that the different dorsal colorations were transient external clues indicating the immediate past environment of a fish, either freshwater or saltwater. The unique coloration fortuitously lasted long enough during the prespawning period to provide the evidence needed for initial separation of the two subgroups prior to examination by elemental microchemical analyses. However, the evidence provided by the Tucker-3 multiway analysis suggests that an individual fish may change behavior to overwinter at a location different from the previous year. In this manner, the otolith microchemical signature as analyzed by this multi-way model reveals the life-long record of the migratory pattern currently not available by any other method.

4. Conclusions

Exploratory analysis of trace elements from hard tissues in biological organisms such as otoliths can reveal patterns that reflect the life history and long-term fluctuations in the chemical environment of the organism. In this study, it has been shown that patterns in the trace elements of otoliths from Shubenacadie striped bass reflect the long-term migratory patterns of individual fish. Despite the small number of fish used in this study, clear trends in Sr/Ca ratios aided significantly in the classification of fish. Blackback fish that overwintered in the fresh headwater Shubenacadie Lake had significantly different levels of trace elements in otoliths with markedly higher levels Sr/Ca ratios compared to greenback fish that overwinter in saline habitats, in good agreement with prior research involving other fish species [12,15, 19,20]. Shubenacadie striped bass otoliths at age 0, regardless of fish color, had trace element compositions similar to mature greenback fish, which is in good agreement with known habits of this species: Juveniles tend to stay in brackish coastal waters until 1–2 years of age [1].

After age 0, trace elements in Shubenacadie striped bass otoliths provided a permanent record of fish habitat; freshwater versus saltwater. The trace element record in otoliths from several individuals suggested that a significant portion of these fish switch between fresh or saltwater overwintering conditions during later years of life. This result has not been experimentally validated in this study; however, previous research on trace elements in otoliths from other species of fish have demonstrated that Sr/Ca ratios can be used to discriminate between fish that migrate or originate from freshwater versus saltwater habitats.

Besides Sr/Ca ratios, other ratios were discovered that exhibited significant variability in Shubenacadie striped bass. Specifically, Cr/Ca and Sr/Ca ratios appeared to be inversely correlated, but only in greenback fish. When all nine fish were considered, the trace element ratios Cr/Ca, Mg/Ca, and Mn/Ca, exhibited correlated behavior. In addition, the ratio, S/Ca, exhibited unique behavior. At the present time, the underlying causes of the observed correlations and unique behavior are not known; however, these results suggest future studies might be designed to investigate them further.

Acknowledgements

Funding for this project was provided by a faculty grant from ECU's Research/Creative Activity Grants Committee to R. Rulifson. We thank Sam Wang of Elemental Research, Vancouver, BC for performing LA-ICP/MS sample analysis.

References

[1] R.A. Rulifson, M.J. Dadswell, Life history and population characteristics of striped bass in Atlantic Canada, Trans. Am. Fish. Soc. 124 (1995) 477–507.
[2] R.A. Rulifson, K.A. Tull, Striped bass spawning in a tidal bore

river: the Shubenacadie estuary, Atlantic Canada, Trans. Am. Fish. Soc. 128 (1999) 613–624.
[3] J. Bergeron, J. Brousseau, Guide des poissons d'eau douce du Quebéc, Ministére du Loisir, de la Chasse et de la Pêche, Direction générale de la faune, Quebéc, 1983.
[4] H. Beaulieu, Rapport sur la situation du bar rayé (*Morone saxatilis*), Faune et flore à protéger au Quebéc, Association des Biologistes du Quebéc, Quebéc, 1985, Publication 7.
[5] J.M. Kalish, Otolith microchemistry: validation of the effects of physiology, age and environment on otolith composition, J. Exp. Mar. Biol. Ecol. 132 (1989) 151–178.
[6] C. Papadopoulou, G.D. Kanias, E. Moraitopoulou-Kassimati, Trace element content in fish otoliths in relation to age and size, Marine Pollut. Bull. 11 (1980) 68–72.
[7] J.S. Edmonds, N. Caputi, M. Morita, Stock Discrimination by trace-element analysis of otoliths of orange roughy (*Hoplostethus atlanticus*), a deep-water marine teleost, Aust. J. Mar. Freshwater Res. 42 (1991) 383–389.
[8] J.S. Gunn, J.R. Harrowfield, C.H. Proctor, R.E. Thresher, Electron microprobe analysis of shish otoliths—evaluation of techniques for studying age and stock discrimination, J. Exp. Mar. Biol. Ecol. 152 (1992) 1–36.
[9] D.H. Secor, J.M. Dean, S.E. Campana, Recent Developments in Fish Otolith Research, Univ. South Carolina Press, Columbia, SC, 1994, 735 pp.
[10] R.L. Radthke, D.J. Shafer, Environmental sensitivity of fish otolith microchemistry, Aust. J. Mar. Freshwater Res. 43 (1992) 935–951.
[11] S.E. Campana, J.D. Neilson, Microstructure of fish otoliths, Can. J. Fish. Aquat. Sci. 42 (1985) 1014–1032.
[12] J.M. Kalish, Use of otolith microchemistry to distinguish the progeny of sympatric anadromous and non-anadromous salmonids, Fish. Bull. 88 (1990) 657–666.
[13] C.C. Coutant, C.H. Chen, Strontium microstructure in scales of freshwater and estuarine striped bass (*Morone saxatilis*) detected by laser ablation mass spectrometry, Can. J. Fish. Aquat. Sci. 50 (1993) 1318–1323.
[14] A.J. Fowler, S.E. Campana, C.M. Jones, S.R. Thorrold, Experimental assessment of the effect of temperature and salinity on elemental composition of otoliths using laser ablation ICPMS, Can. J. Fish. Aquat. Sci. 52 (1995) 1431–1441.
[15] K.E. Limburg, Otolith strontium traces environmental history of subyearling American shad *Alosa sapidissima*, Mar. Ecol.: Prog. Ser. 119 (1995) 25–35.
[16] D.H. Secor, P.M. Piccoli, Age- and sex-dependent migrations of striped bass in the Hudson River as determined by chemical microanalysis of otoliths, Estuaries 19 (1996) 778–793.
[17] S.R. Thorrold, C.M. Jones, S.E. Campana, Response of otolith microchemistry to environmental variations experienced by larval and juvenile Atlantic croaker (*Micropogonias undulatus*), Limnol. Oceanogr. 42 (1) (1997) 102–111.
[18] E.J. Chesney, B.M. McKee, T. Blanchard, L. Chan, Chemistry of otoliths from juvenile menhaden *Brevoortia patronus*: evaluating strontium, strontium: calcium and strontium isotope ratios as environmental indicators, Mar. Ecol.: Prog. Ser. 171 (1998) 261–273.
[19] R. Kafemann, S. Adlerstein, R. Neukamm, Variation in otolith strontium and calcium ratios as an indicator of life-history strategies of freshwater fish species within a brackish water system, Fish. Res. 46 (2000) 313–325.
[20] D.H. Secor, J.R. Rooker, Is otolith strontium a useful scalar of life cycles in estuarine fishes? Fish. Res. 46 (2000) 359–371.
[21] R.E. Thresher, C.H. Proctor, J.S. Gunn, An evaluation of electron-probe microanalysis of otoliths for stock delineation and identification of nursery areas in a southern temperate groundfish, *Nemadactylus macropterus* (Cheilodactylidae), Fish. Bull. 92 (1994) 817–840.
[22] S.E. Campana, G.A. Chouinar, J.M. Hanson, A. Frechet, J. Brattey, Otolith elemental fingerprints as biological tracers of fish stocks, Fish. Res. 46 (2000) 343–357.
[23] S.E. Campana, A.J. Fowler, C.M. Jones, Otolith elemental fingerprinting for stock identification of Atlantic Cod (*Gadus morhua*) using laser ablation ICPMS, Can. J. Fish. Aquat. Sci. 51 (1994) 1942–1950.
[24] J.S. Edmonds, M.J. Moran, N. Caputi, M. Morita, Trace elements analysis of fish sagittae as an aid to stock identification: pink snapper (*Chrysophrys auratus*) in western Australian waters, Can. J. Fish. Aquat. Sci. 46 (1989) 50–54.
[25] J.S. Edmonds, R.C.J. Lenanton, N. Caputi, M. Morita, Trace elements in the otoliths of yellow-eye mullet (*Aldrichetta forsteri*) as an aid to stock identification, Fish. Res. 13 (1992) 39–51.
[26] S.R. Thorrold, C.M. Jones, P.K. Swart, T.E. Targett, Accurate classification of juvenile weakfish *Cynoscion regalis* to estuarine nursery areas based on chemical signatures in otoliths, Mar. Ecol.: Prog. Ser. 173 (1998) 165–253.
[27] L.R. Tucker, Some mathematical notes on three-mode factor analysis, Psychometrika 31 (1966) 279–311.
[28] R.A. Harshman, Foundations of the PARAFAC procedure: model and conditions for an 'explanatory' multi-mode factor analysis, UCLA Working Papers in Phonetics 16 (1970) 1–84.
[29] J.D. Carol, J. Chang, Analysis of individual differences in multidimensional scaling via an N-way generalization of 'Eckart–Young' decomposition, Psychometrica 35 (1970) 283–319.
[30] B.K. Lavine, Chemometrics, Anal. Chem. 70 (1998) 209R–228R.
[31] P.J. Gemperline, K.H. Miller, T.L. West, J.E. Weinstein, J.C. Hamilton, J.T. Bray, Principal component analysis, trace elements, and blue crab shell disease, Anal. Chem. 64 (1992) 523A–532A.
[32] R. Bro, Multi-way analysis in the food industry: models, algorithms and applications, Doctoral Thesis, Royal Veterinary and Agricultural University, Denmark, 1998.
[33] L. Munck, L. Nørgaard, S.B. Engelsen, R. Bro, C.A. Andersson, Chemometrics in food science—a demonstration of the feasability of a highly exploratory, inductive evaluation strategy of fundamental scientific significance, Chemom. Intell. Lab. Syst. 44 (1998) 31–60.
[34] P. Barbieri, C.A. Andersson, D.L. Massart, S. Predonzani, G. Adami, E. Reisenhofer, Modeling bio-geochemical interactions in the surface waters of the Gulf of Trieste by 3-way PCA, Anal. Chim. Acta 398 (1999) 227–235.

[35] P. Paatero, C.A. Andersson, Further improvements of the speed of the Tucker-3 three-way algorithm, Chemom. Intell. Lab. Syst. 47 (1999) 17–20.
[36] P.M. Kroonenberg, J. de Leeuw, Principal component analysis of three-mode data by means of alternating least squares algorithms, Psychometricka 45 (1980) 69–97.
[37] P.M. Kroonenberg, Three-mode principal component analysis, Theory and Applications, DSWO Press, Leiden, The Netherlands, 1983.
[38] L.M. Paramore, R.A. Rulifson, Dorsal coloration as an indicator of different life history patterns for striped bass within a single watershed of Atlantic Canada, Trans. Am. Fish. Soc. (2001) 663–673.